

## THEORETICAL UNDERSTANDING OF MORPHOLOGICAL DISTRIBUTION OF HYDROGEN IN AMORPHOUS CALCIUM SILICATE HYDRATE

Chongsong Zhou<sup>a,\*</sup> and Lilin Lu<sup>b</sup>

<sup>a</sup>Department of Chemistry Biology & Environmental Engineering, Hunan Provincial Key Laboratory of Xiangnan Rare-Precious Metals Compounds and Applications, Xiangnan University, Chenzhou City, Hunan Province, People's Republic of China

<sup>b</sup>State Key Laboratory of Refractories and Metallurgy, Wuhan University of Science and Technology, Wuhan City, Hubei Province, People's Republic of China

Recebido em 08/01/2020; aceito em 28/04/2020; publicado na web em 15/06/2020

Determining the morphological distribution of hydrogen atoms in calcium silicate hydrate phase (C-S-H) is of great concern but challenging. In this work, based on the stoichiometric composition of  $(\text{CaO})_{1.7}(\text{SiO}_2)(\text{H}_2\text{O})_{1.8}$ , a series of amorphous  $\text{Ca}_{1.7}\cdot\text{Si}(\text{O})_{3.7-x}\cdot(\text{OH})_{2x}\cdot(\text{H}_2\text{O})_{1.8-x}$  models are constructed using Monte Carlo method, where  $x$  represents the molar number of dissociated  $\text{H}_2\text{O}$  molecules ( $x \in 0 \sim 1.8$ ). A molecular dynamics simulation has been performed with the ClayFF force field. The analysis of  $Q^n$ , radial distribution function (RDF), coordinate number (CN), mean chain length (MCL), mean square displacement (MSD), elastic modulus ( $M$ ), and Young's modulus ( $E$ ) are used to explore the microstructure, hydrogen atom distribution and mechanical properties. The results demonstrate that the proportions of hydrogen atoms in Ca-OH, Si-OH, and  $\text{H}_2\text{O}$  are about 26%~45%, 13%~22%, and 61%~33%, respectively. The calculated microstructure parameters and mechanical properties, especially for C-S-H models with  $x$  of 0.7~1.2, are in good agreement with those reported previously in theoretical and experimental works, indicative of the excellent rationality of our theoretical C-S-H models. The simulated results of this work provides a new strategy of constructing theoretical C-S-H model, which might be suitable for studying the doping behavior of metal oxides or metal salts in C-S-H.

Keywords: calcium silicate hydrate (C-S-H); morphological distribution; molecular dynamics simulation; hydrogen atoms; amorphous.

### INTRODUCTION

As the core component of cement gels, Calcium-Silicate-Hydrated (C-S-H) accounts for 60%~70% of the cement mass. The chemical composition of C-S-H can be expressed as  $(\text{CaO})_{1.7}(\text{SiO}_2)(\text{H}_2\text{O})_{1.8}$ , determined by small-angle neutron diffraction and  $x$ -ray diffraction techniques.<sup>1</sup> At least three types of hydrogen atoms in C-S-H (i.e., free OH, confined OH and  $\text{H}_2\text{O}$ ) were characterized by two-dimensional NMR technology,<sup>2,3</sup> but their proportions in C-S-H remain unclear.

The coordination state between OH and Si (or Ca) atoms in C-S-H is also arguable. Some experimental studies demonstrated that the percentage of hydrogen bonding between  $\text{SiO}_4$  and  $\text{SiO}_3\text{-OH}$  was 38.14%<sup>4</sup> and the Si-OH bond appear in  $Q^1$  or the non-bridged oxygen of  $Q^2$ .<sup>5</sup> The Si-OH content decreases with the increase of the mole ratio of Ca atoms to Si atoms (C/S) in C-S-H.<sup>5</sup> Si-OH bond disappears at high Ca/Si ratio ( $C/S > 1.2$ ), while Ca-OH bond start appearing at high C/S ratio ( $C/S > 1.3$ ).<sup>6,7</sup> Computational study found that the Si-O...Ca bond might hydrolysis to form a Si-OH bond and a Ca-OH bond at C/S ratio of 1.3,<sup>8</sup> and the number of Si-OH bonds per Si atom was about 0.25 and 0.1 when the C/S ratio equals to at 1.4 and 2.0, respectively.<sup>9</sup>

The molecular simulation technology provides a new method to explore the bonding state of hydrogen atoms in C-S-H on the atomic scale. It is critical and challenging to construct a reasonable theoretical C-S-H model to perform theoretical simulations. In previous works, two C-S-H models were used to investigate the microstructure and mechanical properties of cement paste. One is sandwiched and layer-ordered C-S-H model based on Tobermorite/Calcium hydroxyl (T/CH) or Tobermorite/Jennite (T/J) crystal,<sup>10</sup> the other is amorphous

C-S-H model formed from the polymerization of  $\text{Si}(\text{OH})_4$ ,  $\text{Ca}(\text{OH})_2$  and  $\text{H}_2\text{O}$ .<sup>9</sup>

The former has successfully elucidated the experimental results such as the mechanical properties of C-S-H and the effect of C/S ratio on mechanical properties, and has been proved to be suitable for studying the surface structure and the properties of C-S-H.<sup>11,12</sup> However, the infinitely linked  $\text{SiO}_4$  tetrahedron chains in this C-S-H model are inconsistent with the fact that the dimers and pentamers are dominant in the actual cement gels. Pellenq *et al.*<sup>13</sup> manually removed some  $\text{SiO}_2$  units from the T/CH models to match the experimental  $Q^n$  distribution, the density and elastic modulus of C-S-H. Lack of universality is the main disadvantage of this method, which relies heavily on individual expertise and experience.

Dolado *et al.*<sup>9</sup> has used the latter model to simulate the formation process of C-S-H and hydrogen bonding that was observed in the experimental research, however, this theoretical work led to excessive mole ratio of water molecules to Si atoms (H/S), which influenced the polymerization of  $\text{SiO}_4$  tetrahedra and resulted in excessively high  $Q^0$  at  $C/S=2.0$ .

As proved by previous works, theoretical study based on an ideal model without artificial modification was desirable for understanding the experimental results about the microstructure and mechanical properties of C-S-H. In this work, molecular dynamics simulation was performed on the basis of amorphous C-S-H models, which was derived from the random combination of some atomic units such as Ca, Si, O, OH, and  $\text{H}_2\text{O}$ .<sup>9</sup> During the molecular dynamics studies, ClayFF force field parameters<sup>14,15</sup> were selected to simulate the geometry of the C-S-H model. The microstructure and mechanical properties were analyzed to elucidate the morphological distribution of hydrogen atoms in C-S-H.

\*e-mail: youandi2008@163.com

## COMPUTATIONAL DETAILS

Based on the basic atomic units including Ca, Si, O, OH, and H<sub>2</sub>O, the cubic models of Ca<sub>1.7</sub>•Si•(O)<sub>3.7-x</sub>•(OH)<sub>2x</sub>•(H<sub>2</sub>O)<sub>1.8-x</sub> ( $x$  represents the molar number of dissociated H<sub>2</sub>O molecules,  $x \in 0 \sim 1.8$ , C/S=1.7, H/S=1.8 and a density of 2.604 g cm<sup>-3</sup> in the reference)<sup>1</sup> are constructed by using Monte-Carlo method in Materials Studio software.<sup>16</sup> The detailed numbers of basic atomic units in C-S-H are shown in Table 1.

The ClayFF force field<sup>14</sup> is used to calculate the structure and properties of C-S-H in this work. ClayFF is a set of parameters obtained by fitting a set of simple and characteristic hydrated phases, so that its parameters, like CementFF,<sup>17</sup> have very good transferability.<sup>15</sup> Therefore, it is very beneficial to the bonding and exchange processes between these basic atomic units in CSH model. Moreover, ClayFF has been used to describe the bulk structure of various simple hydroxide and oxyhydroxide phases<sup>15</sup> and the surface behaviors of alkylated quartz<sup>18</sup> successfully.

In ClayFF, the total potential energy comprises four types of interaction as the equation 1:

$$E_{\text{total}} = E_{\text{coul}} + E_{\text{VDW}} + E_{\text{bondstretch}} + E_{\text{anglebend}} \quad (1)$$

where  $E_{\text{bondstretch}}$  only involves the elastic vibration of O-H in OH and H<sub>2</sub>O,  $E_{\text{anglebend}}$  only considers the bending vibration of H-O-H in H<sub>2</sub>O, and the remaining potential energy is described by the non-bonded Coulomb (short range) and van der Waals (long range) interaction. The detailed parameters of the ClayFF force field are listed in Table 1S in Supporting Information.

The atomic types of ClayFF force field are assigned as follows. The cah of 1.0500 charge is used for the Ca atoms, and the st of 2.1000 charge is used for Si atoms. The oh of -0.9500 charge, the o\* of -0.8200 charge and the ob of -1.0500 charge is used for O atoms in OH group, H<sub>2</sub>O and the other part, respectively. The ho of 0.4250 charge and the h\* of 0.4100 charge is used for H atoms in OH and H<sub>2</sub>O, respectively. The species such as CaO, SiO<sub>2</sub>, Ca(OH)<sub>2</sub> and Si(OH)<sub>4</sub> maintain electrical neutrality during ion exchange. The parameters have been used to fully optimize the crystal structure of Jennite,<sup>19</sup> and the average relative deviation between theoretical and experimental unit cell parameters is about 0.39%, indicative of the applicability of the ClayFF force field and the effectiveness of atomic type assignment method in C-S-H simulation.

These C-S-H models are relaxed under NVT ensemble with a step size of 0.2 fs at 298.15 K. The nose-hoover method<sup>20</sup> with Q-ratio of 0.10 is selected to control temperature. The electrostatic and van der Waals interaction are calculated by Ewald addition method.<sup>21</sup> The energy convergence standard is set to 0.01 kcal mol<sup>-1</sup>. The Q<sup>n</sup> change is used to evaluate the adequacy of simulation time (see Table 2S). The mean absolute deviations of Q<sup>n</sup> between 1000 ps simulation and

100 ps simulation are only 1.42% and 1.32% for  $x=0.4$  and  $x=1.5$  C-S-H model, respectively, indicating that 100 ps is sufficient for molecular dynamics (MD) simulations. Therefore, the trajectory of 100 ps simulation is used to analyze the structure parameters (Q<sup>n</sup>, RDF, and CN) and elastic modulus ( $M$ ).

The C-S-H trajectory files after MD simulation are optimized using Discover software, and then the mechanical properties are calculated using ClayFF force field in GULP program.<sup>16</sup> The mean modulus of C-S-H structures at the last 10 ps is reported in this study. All simulations are performed in Material Studio software package<sup>16</sup> and the statistical results of Q<sup>n</sup>, RDF, and CN are calculated by using self-programming codes (see Supporting Information). The distance of 3.2 angstroms is set as the threshold for chain formation *via* SiO<sub>4</sub> tetrahedra polymerization.

## RESULTS AND DISCUSSION

### Polymerization of SiO<sub>4</sub> chain and Q<sup>n</sup>

The polymerization of SiO<sub>4</sub> forming chain, which plays a critical role in cement hydration, is characterized by the Q<sup>n</sup> for the C-S-H models with different  $x$  value, the evolution of Q<sup>n</sup> has been shown in Figure 1.

As for the polymerization process, the simulation results show that all Si atoms can form SiO<sub>4</sub> tetrahedra and thus generate a longer SiO<sub>4</sub> chain. All Ca atoms are dispersed randomly around SiO<sub>4</sub> chains to form layered C-S-H structure (see Figure 1S).<sup>10</sup> The evolution of Q<sup>n</sup> shows that the polymerization process of SiO<sub>4</sub> in C-S-H can quickly reach equilibrium state within 1 ps, whereas this process was reported to more than 500 ps in previous work (see  $h$  in Figure 1).<sup>9</sup> This indicates that the randomly stacked C-S-H model based on the basic atomic units can quickly reach equilibrium state. This can be attributed to the rapid migration of these ionic basic units with ClayFF force field, just as all MD simulations reach convergence in structure within 20 ps.<sup>14,15</sup>

In order to investigate the stability of Q<sup>n</sup> in random C-S-H models, ten original C-S-H models ( $x=1.0$ ) are randomly constructed using the same modeling method, and then are relaxed under the same simulation conditions. All standard deviations of Q<sup>n</sup> being within 2.69% indicates the reliable reproducibility of the modeling method (see Table 3S in Supporting Information).

The calculated Q<sup>0</sup>, Q<sup>1</sup>, Q<sup>2</sup>, and Q<sup>3</sup>+Q<sup>4</sup> range from 14.1% to 44.5%, from 54.7% to 36.4%, from 30.7% to 14.6%, and from 0.4% to 1.5%, respectively (Figure 2). In the experimental works reported by Rawal<sup>2</sup> and Mendes,<sup>22</sup> the values of Q<sup>0</sup>, Q<sup>1</sup>, Q<sup>2</sup>, Q<sup>3</sup>+Q<sup>4</sup> are within 36%~41%, 40%~39%, 24%~20%, 0%, respectively. The computational results also agree with the experimental range of 35-19% for Q<sup>0</sup>, 38%~45% for Q<sup>1</sup>, and 27%~37% for Q<sup>2</sup> in the hydrated products after 3~28 days of C<sub>3</sub>S hydration.<sup>23</sup>

**Table 1.** The number of basic atomic units in Ca<sub>1.7</sub>•Si•(O)<sub>3.7-x</sub>•(OH)<sub>2x</sub>•(H<sub>2</sub>O)<sub>1.8-x</sub>

$x^a$	Ca	Si	O	OH	H <sub>2</sub> O	Density <sup>1</sup>
0.0	340	200	740	0	360	2.604
0.4	340	200	660	160	280	2.604
0.7	340	200	600	280	220	2.604
1.0	340	200	540	400	160	2.604
1.2	340	200	500	480	120	2.604
1.5	340	200	440	600	60	2.604
1.7	340	200	400	680	20	2.604

<sup>a</sup> $x$  is the molar number of dissociated water molecules,  $x=0 \sim 1.8$ .

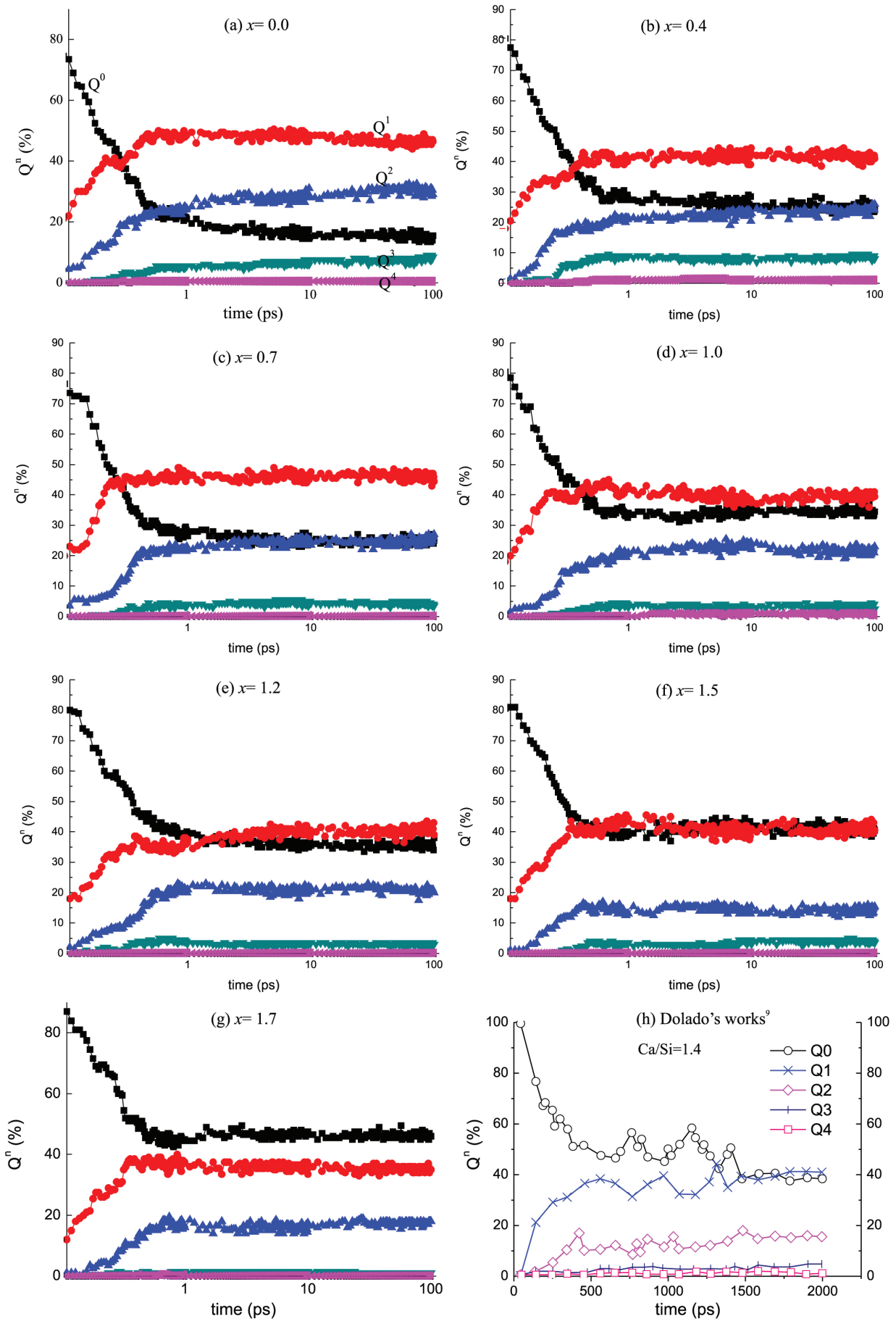


Figure 1. The evolution of  $Q^n$  in C-S-H

Relative to the similar theoretical range of 39.3%~62.0% for  $Q^0$ , 40%~32% for  $Q^1$ , and 16%~4% for  $Q^2$  in C-S-H models with C/S ratios of 1.4~2.0,<sup>9</sup> there are slightly less  $Q^0$  and more  $Q^2$  in this work, indicative of the higher polymerization degree of  $SiO_4$  due to a reasonable H/S ratio. However, there are slightly more  $Q^0$  and less  $Q^1$  than the results of 12% for  $Q^0$ , 67% for  $Q^1$ , and 21% for  $Q^2$  in the cCSH models (C/S=1.7)<sup>24</sup> and the results of 10% for  $Q^0$ , 67% for  $Q^1$ , and 23% for  $Q^2$ .<sup>13</sup> Both of their C-S-H models were characterized by highly hydration and dominant  $Q^1$  because of the artificial remove of  $SiO_2$  based on Tobermorite.

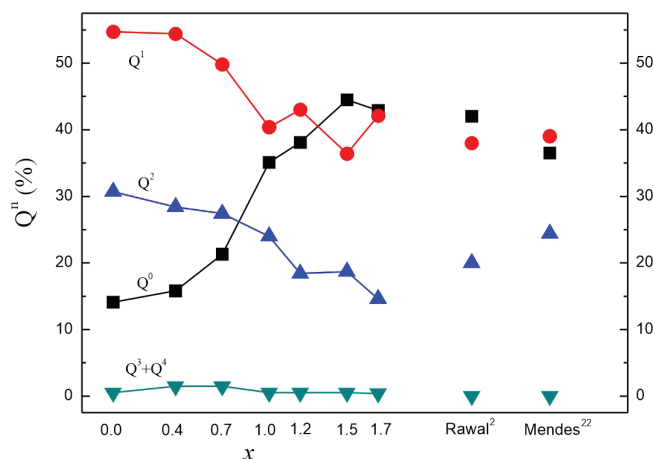


Figure 2. Effect of  $x$  on  $Q^n$

The variation of individual  $Q^n$  in this work is consistent with the evolution process of  $Q^n$ ,<sup>9</sup> where the  $Q^0$  decreases while the  $Q^1$  and  $Q^2$  increase with simulation time. Meanwhile, the value of  $Q^1$  is always greater than that of  $Q^2$  regardless of  $x$ . However, the  $Q^0$  decreases with the increase of  $x$ , for instance, there being  $Q^0 < Q^2 < Q^1$  at  $x=0$ , while the  $Q^0$  being equivalent to the  $Q^2$  at  $x=0.7$ , and even the  $Q^0$  being equivalent to the  $Q^1$  at  $x>1.2$  (Figure 2). It indicates the decrease of water molecules and bridged oxygen atoms in C-S-H with increasing  $x$  does not conducive to the lengthening of  $SiO_4$  chains.

According to the mean chain length= $2 \times (1 + Q^2/Q^1)$ , the calculated MCL within 2.69~3.19 are in excellent agreement with the experimental results of 3.05 for Portland cement slurry<sup>2</sup> and of 3.25 for cement gels doped by slag,<sup>22</sup> indicating that the dimers and pentamers of  $SiO_4$  chains are dominant in this C-S-H governed by a  $3n-1$  rule.

### Microstructural information of C-S-H models

The radial distribution function (RDF) and coordination number (CN) have been calculated to understand the microstructure of C-S-H. The computational results show that the RDF and CN between Ca (or Si) and total O atoms hardly vary with increasing  $x$ , hence the RDF and CN of C-S-H only at  $x=1.0$  is shown in Figure 3. It can be seen from Figure 3 that there exists a clearly localized interaction at an average distance of 1.57 Å for Si-O bond and of 2.47 Å for Ca-O bond. They reproduce the 1.62 Å of Si-O and 2.38 Å of Ca-O for Tobermorite and Jennite, and the 1.60 Å of Si-O and 2.45 Å of Ca-O for cCSH models.<sup>13</sup> Relatively to cCSH models, there is a narrower Si-O peak on the RDF curve in this model, indicating that the bonding between Si and O atoms is more orderly on the short range. The CN of Si-O and Ca-O in the first coordinating layer is 4.0 and 6.0, respectively, indicative of the formation of  $[SiO_4]$  tetrahedron and  $[CaO_6]$  octahedron in this C-S-H. Therefore, the

random C-S-H model based on basic atomic units can reappear well the experimental and theoretical microstructure of C-S-H.

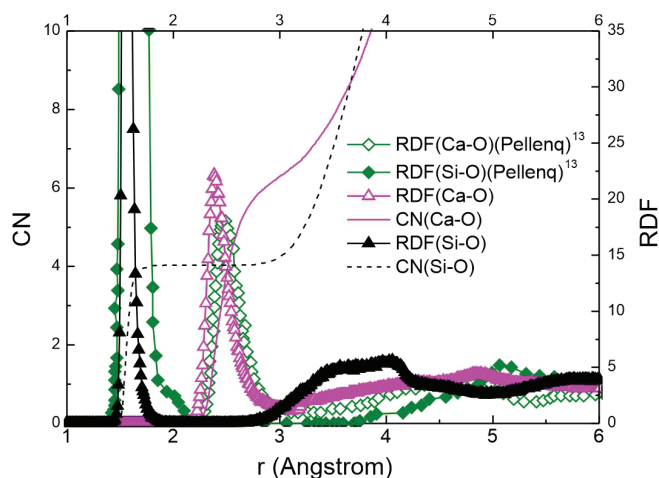


Figure 3. The Radial distribution function (RDF) and coordination number (CN) in the C-S-H of  $x=1.0$

It can be also found from Figure 3 an obvious long-range interaction between Si and O atoms in the range of 3~4.2 Å, which did not emerge in the cCSH models.<sup>13</sup> The RDF and CN between Si and O atoms (including  $O_b$ ,  $O_h$ , and  $O_w$ ) are calculated to explore their long-range interaction as seen in Figure 4. In the first coordination layer, the CN is 2.7 for Si- $O_b$ , 1.2 for Si- $O_h$ , and 0.1 for Si- $O_w$ , indicating that the major of Si atoms coordinate with the bridged O atoms and a small part of Si atoms can form Si-OH bond, while the Si atoms hardly interact with the O atoms of water molecules. There is an inconsiderable second coordination layer between Si and O atoms in the range of 3.0~4.5 Å. The RDF peak at 3.5 Å between Si and the O atoms of OH is closer than that of 4.0 Å between Si and the bridged O atoms. The total CN of Si-O is 16.0 within 4.2 Å (in Figure 3) included 8.0 of Si- $O_b$ , 6.0 of Si- $O_h$ , and 2.0 of Si- $O_w$  (in Figure 4). Therefore, the CN is 4.8 for Si- $O_b$  and 1.9 for Si- $O_w$  in the second layer after subtracting their CN in the first layer, indicating that the number of hydrogen bonds is about 5 for the  $Si_{(1)}-O_{b(2)} \cdots H_{h(3)}-O_{h(4)}$  and  $Si_{(1)}-O_{h(2)}-H_{h(3)} \cdots O_{h(4)}$  interaction and about 2 for the  $Si_{(1)}-O_{b(2)} \cdots H_{w(3)}-O_{w(4)}$  and  $Si_{(1)}-O_{h(2)}-H_{h(3)} \cdots O_{w(4)}$  interaction in the range of 3.0~4.2 Å. The smaller mean square displacement (MSD) of water molecules in C-S-H models can also indicate the existence of these hydrogen bonds (See Figure 2S).

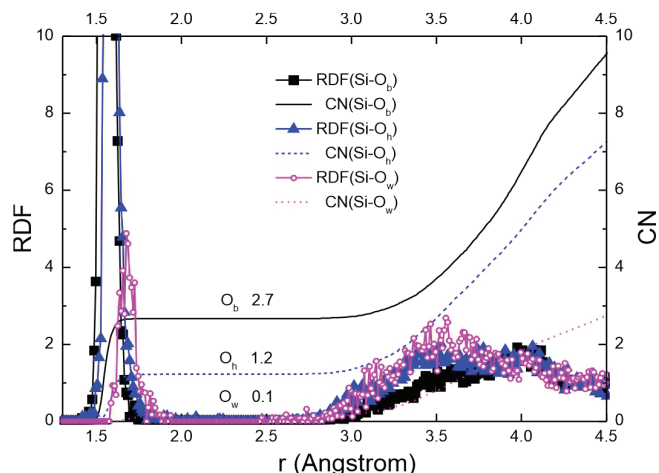


Figure 4. The RDF and CN between Si and three types of O atoms in the C-S-H of  $x=1.0$

### Bonding of OH with Si (or Ca)

In order to investigate in detail the bonding of OH and Si (or Ca), their CN and proportions of various OH in C-S-H are shown in Table 2 (except for the C-S-H model at  $x=0$ ). It can be seen from Table 2, the ratio of the CN between Si (or Ca) and  $O_h$  to the CN between Si (or Ca) and total O increases with the  $x$  (see column *d*). Therefore, the percentage of Si (or Ca) linking with OH gets bigger (see column *c*). Similarly, the number of Si-OH (or Ca-OH) bond increases with increasing  $x$ , and the average number increases from 1.29 to 2.34 per Si atom for Si-OH bond while it ranges from 1.34 to 2.96 per Ca atom for Ca-OH bond (see column *e*).

Based on the analysis of CN and charge balance, their distribution ratios of OH between Si-OH and Ca-OH are listed in Table 2. Regardless of the  $x$  in the C-S-H models, there are about 31% of OH linked to Si atoms, and each OH is localized around only one Si atom. Whereas about 67% of OH will be interacted with Ca atoms, and two Ca atoms share one OH group on average. It is consistent with the results that most of the OH interacts with Ca atoms in C-S-H (see Figure 3S).<sup>2,5</sup> Moreover, the fracture of  $SiO_4$  chain in cement pastes may cause the dissociation of  $H_2O$  molecules to form the Si-OH and Ca-OH,<sup>13</sup> and the thermogravimetric results have also shown that the weightless process occurred at 200~300 °C corresponds to the dehydration process of Si-OH bonds.<sup>25,26</sup> Therefore, it is reasonable to emerge Si-OH in C-S-H.

The Ca-OH/Ca ratio ranges from 0.33 to 1.37 in this work (see column *j*), indicating that the charges of about 15-64% Ca atoms in C-S-H are balanced by the OH groups. Similarly, the experimental Ca-OH/Ca ratio of 0.46 means the charges of 23% Ca atoms being balanced by the OH groups for the C-S-H with a C/S ratio of 1.7.<sup>27</sup> The simulated Ca-OH/Ca ratios of 0.55~0.95 when  $x=0.7\sim 1.2$  are closely consistent with their experimental ratio of 0.46, and this subtle difference can be attributed to a different H/S ratio (1.8 vs 1.34).

The ratios of H (or O) atoms in Ca-OH, Si-OH, and  $H_2O$  to total H (or O) atoms are calculated to study their coordination status in C-S-H as shown in Table 3. Based on the data of O atom distribution,<sup>28</sup> the ratio of H atoms in Ca-OH, Si-OH, and  $H_2O$  is in the range of 34%~46%, 9%~25%, and 31%~54%, respectively, while it is 15%~64%, 7%~29%, and 7%~78% in this simulation, respectively. Obviously, the larger simulated distribution range of H atoms covers the experimental results obtained from the various C-S-H samples with a C/S ratio from 1.54 to 1.85. An amorphous C-S-H model of  $x=0.4\sim 1.7$ , 0.7~1.5, and 0.7~1.2 is suitable for the precise demonstration of Si-OH, Ca-OH, and  $H_2O$ , respectively. Therefore, it is suggested that a wide applicability of this modeling.

Based on the above discussion of the CN and charge balance between OH and Si (or Ca), it can be concluded that the C-S-H models of  $x=0.7\sim 1.2$  may completely reproduce the distribution of three types of OH in actual C-S-H.

### Mechanical properties of C-S-H

The higher-order properties such as elastic constants ( $E$ ) are often used to investigate the microstructure of materials. The calculated mechanical properties of C-S-H models are shown in Table 4.

The calculated elastic modula ( $M$ ) and Young's modula ( $E$ ) of C-S-H models vary within 53~69 GPa and 48~63 GPa, respectively. For the C-S-H model ( $x=1.2$ ), both  $M$  and  $E$  are exactly consistent with the values reported in theoretical works<sup>13,29</sup> and experimental works.<sup>30</sup> In addition, these simulated elastic modula of C-S-H models (C/S=1.7) are closer to that of Jennite (C/S=1.5), but are far from that of Tobermorite-14 (C/S=0.83).

### Reasonable range of $x$

It can be concluded that the effects of  $x$  value in C-S-H models

**Table 2.** (a) The bonding between Si and OH; (b) The bonding between Ca and OH

(a)									
$x^a$	OH/H (%) <sup>b</sup>	Si-OH/Si (%) <sup>c</sup>	CN(Si- $O_h$ )/CN(Si-O) <sup>d</sup>	Si-OH per Si <sup>e</sup>	Si-OH/OH (%) <sup>f</sup>	OH_Si <sup>g</sup>	SiOH/OH (%) <sup>h</sup>	Si-OH/H <sup>i</sup>	
0.4	22	37	0.12	1.29	59	1.00	29	0.07	
0.7	39	59	0.22	1.50	63	1.02	31	0.13	
1.0	56	74	0.33	1.81	66	1.01	33	0.18	
1.2	67	78	0.38	1.93	62	1.02	31	0.21	
1.5	83	89	0.47	2.11	61	1.02	31	0.25	
1.7	94	90	0.53	2.34	61	1.01	31	0.29	
(b)									
$x^a$	OH/H (%) <sup>b</sup>	Ca-OH/Ca (%) <sup>c</sup>	CN(Ca- $O_h$ )/CN(Ca-O) <sup>d</sup>	Ca-OH per Ca <sup>e</sup>	Ca-OH/OH (%) <sup>f</sup>	OH_Ca <sup>g</sup>	CaOH/OH (%) <sup>h</sup>	Ca-OH/H <sup>i</sup>	Ca-OH/Ca <sup>j</sup>
0.4	22	52	0.12	1.34	99	2.10	69	0.15	0.33
0.7	39	71	0.19	1.61	99	2.05	67	0.26	0.55
1.0	56	82	0.26	1.93	99	2.04	66	0.37	0.77
1.2	67	88	0.34	2.30	98	2.11	67	0.45	0.95
1.5	83	94	0.41	2.62	99	2.05	68	0.57	1.21
1.7	94	97	0.48	2.96	99	2.07	68	0.64	1.37
The experimental result of C-S-H of C/S = 1.7 and H/S = 1.34 by Thomas <i>et al.</i> <sup>27</sup>									0.46

<sup>a</sup>The molar number of dissociated  $H_2O$  molecules in C-S-H models; <sup>b</sup>The percentage of H atoms in OH to total H atoms, %; <sup>c</sup>The percentage of Si (or Ca) atoms formed Si-OH (or Ca-OH) bond to total Si (or Ca) atoms, %; <sup>d</sup>The ratio of the coordination number between Si (or Ca) and  $O_h$  atomic type to the total coordination number between Si (or Ca) and O; <sup>e</sup>The average number of Si-OH (or Ca-OH) bond per Si (or Ca) atom; <sup>f</sup>The percentage of OH interacted with Si (or Ca) to total OH, including long range interaction, %; <sup>g</sup>The average number of Si (Ca) atoms interacted with OH per OH; <sup>h</sup>The distributed ratio of OH between Si-OH and Ca-OH, calculated by the coordination number between OH and Si (or Ca), %; <sup>i</sup>The molar ratio of H atoms in the form of Si-OH (or Ca-OH) to total H atoms; <sup>j</sup>The molar ratio of Ca-OH bonds to total Ca atoms, reflecting the molar ratio of Ca required OH to balance its charge to the total Ca.

**Table 3.** The distribution of O and H atoms in C-S-H

C/S	Raw materials	Ca-OH <sup>25</sup>	Si-OH <sup>25</sup>	H <sub>2</sub> O <sup>25</sup>	Ca-OH/H <sup>a</sup>	Si-OH/H <sup>a</sup>	H <sub>2</sub> O/H <sup>a</sup>
1.85	C <sub>2</sub> S+H <sub>2</sub> O	24	8	12	43	14	43
1.85	C <sub>2</sub> S+SiO <sub>2</sub>	34	10	15	46	14	41
1.77	C <sub>2</sub> S+H <sub>2</sub> O	22	8	15	37	13	50
1.70	CaO+SiO <sub>2</sub>	25	5	12	46	9	44
1.70	C <sub>2</sub> S+SiO <sub>2</sub>	29	10	23	34	12	54
1.56	C <sub>2</sub> S+H <sub>2</sub> O	18	6	9	43	14	43
1.54	CaO+SiO <sub>2</sub>	23	13	8	44	25	31
Experimental range					34~46	9~25	31~54
MD results in present work					15~64	7~29	7~78

<sup>a</sup>The calculation results based on the percentage of O atoms.<sup>25</sup>

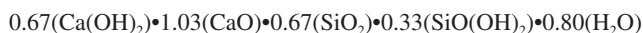
**Table 4.** The mechanical properties of C-S-H

model ( <i>x</i> )	Hill's Bulk Modulus ( <i>K</i> ) (GPa)	Hill's Shear Modulus ( <i>G</i> ) (GPa)	Elastic Modulus ( <i>M</i> ) <sup>a</sup> (GPa)	Young's Modulus ( <i>E</i> ) (GPa)
0.0	51.7	17.7	54.3	47.8
0.4	53.9	20.7	61.8	55.1
0.7	53.6	19.7	59.4	52.7
1.0	51.9	18.8	56.8	50.3
1.2	51.6	24.4	69.4	63.3
1.5	46.3	17.9	53.4	47.7
1.7	51.2	19.9	59.3	52.9
Jennite	43.0	26.0	69.0	66.0
Tobermorite-14	46.0	39.0	94.0	91.0
cCSH (core-shell force field) <sup>13</sup>	49.5	22.7	64.9	63.0
cCSH (CSHFF force field) <sup>29</sup>	50.5	21.7	63.1	57.0
C-S-H (indentation experiment) <sup>30</sup>	-	-	65.0	59.7

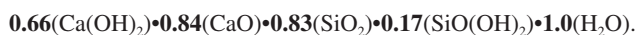
<sup>a</sup>The alculated results with  $M = 4G(3K+G)/(3K+4G)$ .

on the structural and mechanical properties are different. The *x* value show negligible influence on SiO<sub>4</sub> polymerization, RDF, CN between Si (or Ca) and total O atoms, mean number of OH groups connected to individual Si (or Ca) atoms, the distribution proportion of OH in Si (or Ca) atoms, and elastic modulus (*M* and *E*). These results are consistent with those reported in literatures.<sup>9,13,22-24,29,30</sup> However, Q<sup>n</sup> distribution, MCL, polymerization degree of SiO<sub>4</sub>, and CN between Si (or Ca) atoms and three types of OH are distinctly influenced by the *x* value. When *x* varies in the range of 0.7~1.2, these results agree well with the reported theoretical and experimental results.<sup>9,13,22-24,27,31</sup> Therefore, the amorphous (CaO)<sub>1.7</sub>(SiO<sub>2</sub>)(OH)<sub>2x</sub>(H<sub>2</sub>O)<sub>1.8-x</sub> (*x*=0.7~1.2) models constructed by using the Monte Carlo method based on basic atomic units are rational for investigation of the microstructure and mechanical properties of C-S-H.

For the models with different *x* value, the percentage of H atoms in Ca-OH, Si-OH, and water molecules for C-S-H are about 26%~45%, 13%~22%, and 61%~33%, respectively. The chemical formula for the C-S-H of *x*=1.0 can be expressed as:



This chemical formula is similar to that of natural Jennite:<sup>30</sup>



Therefore this amorphous C-S-H model in this work is characterized by Jennite-like microstructure.

## CONCLUSIONS

It is of great significance to grasp the existing form and distribution of hydrogen in C-S-H for understanding the microstructure and mechanical properties of C-S-H. In this work, a new strategy of C-S-H models construction based on the basic units of Ca, Si, O, OH and H<sub>2</sub>O is presented to explore the microstructure of C-S-H and hydrogen atom distribution in C-S-H by combining MD simulation with ClayFF force field. It has been shown that the amorphous C-S-H models can reach equilibrium quickly and reproduce the microstructure and mechanical properties of C-S-H. This provides a new idea for constructing theoretical model for computational study of C-S-H on a larger molecular scale.

For the Ca<sub>1.7</sub>•Si•(O)<sub>3.7-x</sub>•(OH)<sub>2x</sub>•(H<sub>2</sub>O)<sub>1.8-x</sub> model (*x*=0.7~1.2), the simulated Q<sup>n</sup>, RDF, CN and elastic modulus are consistent with those reported in previous theoretical and experimental works. In the C-S-H, the percentages of hydrogen atom in Ca-OH, Si-OH, and H<sub>2</sub>O are determined to be about 26%~45%, 13%~22%, and 61%~33%, respectively.

The chemical structural formula of C-S-H of *x*=1.0 can be expressed as:

$0.67(\text{Ca}(\text{OH})_2) \cdot 1.03(\text{CaO}) \cdot 0.67(\text{SiO}_2) \cdot 0.33(\text{SiO}(\text{OH})_2) \cdot 0.80(\text{H}_2\text{O})$ ,

which excellent matches the structural characteristics of natural jennite ( $C/S=1.5$ ).

#### SUPPLEMENTARY MATERIAL

The parameters in the ClayFF force field, the results about the adequacy of simulation time and reproducibility of modelling method, the layered C-S-H structure, the MSD of water molecules in deferent C-S-H models, the proportional variation of three types of H atoms in C-S-H, and the *awk* code for calculating  $Q^n$  in this study are available on <http://quimicanova.s bq.org.br> in the form of a PDF file with free access.

#### ACKNOWLEDGEMENTS

This manuscript was funded by the Talent Introduction Science Research Fund of Xiangnan University.

#### REFERENCES

- Allen, A. J.; Thomas, J. J.; Jennings, H. M.; *Nat. Mater.* **2007**, *4*, 311.
- Rawal, A.; Smith, B. J.; Athens, G. L.; Edwards, C. L.; Roberts, L.; Gupta, V.; Chmelka, B. F.; *J. Am. Chem. Soc.* **2010**, *21*, 7321.
- Thomas, J. J.; FitzGerald, S. A.; Neumann, D. A.; Livingston, R. A.; *J. Am. Ceram. Soc.* **2001**, *8*, 1811.
- Dharmawardhana, C.; Bakare, M.; Misra, A.; Ching, W. Y.; *J. Am. Ceram. Soc.* **2016**, *6*, 2120.
- Cong, X. D.; Kirkpatrick, R. J.; *Adv. Cem. Based Mater.* **1996**, *3*, 133.
- Yu, P.; Kirkpatrick, R. J.; Poe, B.; McMillan, P.F.; Cong, X. D.; *J. Am. Ceram. Soc.* **1999**, *3*, 742.
- Yang, J.; Hou, D. S.; Ding, Q. J.; *ACS Sustainable Chem. Eng.* **2018**, *7*, 9403.
- Zhou, Y.; Hou, D.; Geng, G.; Feng, P.; Yu, J.; Jiang, J.; *Phys. Chem. Chem. Phys.* **2018**, *12*, 8247.
- Dolado, J. S.; Griebel, M.; Hamaekers, J.; *J. Am. Ceram. Soc.* **2007**, *90*, 3938.
- Richardson, I. G.; *Cem. Concr. Res.* **1999**, *8*, 113.
- Rimsza, J. M.; Jones, R. E.; Criscenti, L. J.; *Langmuir* **2017**, *15*, 3882.
- Mitra, N.; Sarkar, P. K.; Prasad, D.; *Phys. Chem. Chem. Phys.* **2019**, *21*, 11416.
- Pellenq, R. J.-M.; Kushima, A.; Shahsavari, R.; Van Vliet, K. J.; Buehle, M. J.; Yip, S.; Ulm, B. S.; *Proc. Natl. Acad. Sci. U. S. A.* **2009**, *38*, 16102.
- Cygan, R. T.; Liang, J. J.; Kalinichev, A. G.; *J. Phys. Chem. B* **2004**, *4*, 1255.
- Mishra, R. K.; Mohamed, A. K.; Geissbühler, D.; Manzano, H.; Jamil, T.; Shahsavari, R.; Kalinichev, A.G.; Galmarini, S.; Tao, L.; Heinz, H.; Pellenq, R.; van Duin, A. C.T.; Parker, S. C.; Flatt, R. J.; Bowen, P.; *Cem. Concr. Res.* **2017**, *102*, 68.
- Accelrys Software inc.; *Materials Studio Release Notes, Release 5.0*, San Diego, Accelrys Software Inc., 2009.
- Galmarini, S.; Aimable, A.; Ruffray, N.; Bowen, P.; *Cem. Concr. Res.* **2011**, *12*, 1330.
- Abramov, A.; Iglauer, S.; *Langmuir* **2019**, *17*, 5746.
- Bonaccorsi, E.; Merlino, S.; Taylor, H. F. W.; *Cem. Concr. Res.* **2004**, *9*, 1481.
- Nose, S.; *Mol. Phys.* **1984**, *2*, 255.
- Karasawa, N.; Goddard, W. A.; *Macromolecules* **1992**, *26*, 7268.
- Mendes, A.; Gates, W. P.; Sanjayan, J. G.; Collins, F.; *Mater. Struct.* **2011**, *10*, 1773.
- Goñi Elizalde, S.; Puertas, F.; Hernández, M. S.; Palacios, M.; Guerrero, A.; Dolado, J. S.; Zanga, B.; Baroni, F.; *J. Therm. Anal. Calorim.* **2010**, *102*, 965.
- Qomi, M. J. A.; Ulm, F. J.; Pellenq Roland, J. M.; *J. Am. Ceram. Soc.* **2012**, *3*, 1128.
- Faucon, P.; Delaye, J. M.; Virlet, J.; Jacquinet, J. F.; Adenot, F.; *Cem. Concr. Res.* **1997**, *10*, 1581.
- Hidalgo, A.; Petit, S.; Domingo, C.; Alonso, C.; Andrade, C.; *Cem. Concr. Res.* **2007**, *1*, 63.
- Thomas, J. J.; Chen, J. J.; Jennings, H. M.; Neumann, D. A.; *Chem. Mater.* **2003**, *20*, 3813.
- Cong, X. D.; Kirkpatrick, R.; *J. Am. Ceram. Soc.* **1996**, *6*, 1585.
- Shahsavari, R.; Pellenq Roland, J. M.; Ulm, F. J.; *Phys. Chem. Chem. Phys.* **2011**, *13*, 1002.
- Constantinides, G.; Ulm, F.-J.; *J. Mech. Phys. Solids* **2007**, *1*, 64.
- Wang, L.; He, Z.; Zhang, B.; Cai, X. H.; *J. Chin. Ceram. Soc.* **2010**, *11*, 2212.